

Radial selection rule for the breathing mode of a harmonically trapped gas

Miguel Tierz^{1,*}

¹*Shanghai Institute for Mathematics and Interdisciplinary Sciences
Block A, International Innovation Plaza, No. 657 Songhu Road, Yangpu District,
Shanghai, China*

Within a fixed hyperangular channel $s > 0$ of a harmonically trapped system, the $1/R^2$ perturbation is absorbed exactly into a shift of the channel parameter, $s \rightarrow s_\eta$, so the single-channel model remains a harmonic oscillator with a shifted inverse-square term: radial gaps stay at $2\hbar\omega$ exactly and no monopole spectral weight appears at forbidden frequencies at any order. The first-order cancellation is also proved independently by a compact algebraic argument in which the ket and bra contributions cancel pairwise; this is the main new result. Substituting single-channel quantities into the established m_1/m_{-1} sum-rule bound yields Q^{-1} scaling of the sum-rule estimate ($Q \equiv 2q + s + 1$, q the radial quantum number) with an explicit coefficient; its finite-temperature average has a low- T plateau and a $1/T$ high- T tail. All results hold for any real $s > 0$. The Laguerre polynomial identities extend formally to three dimensions, but exact 3D results show q -dependent contact corrections along $SO(2, 1)$ ladders, so the physical interpretation there requires a separate derivation.

I. INTRODUCTION

The monopole (breathing) mode of a harmonically trapped gas is a precision probe of symmetry and of controlled symmetry breaking [1–4]. In any spatial dimension, an $SO(2, 1)$ dynamical symmetry pins the breathing frequency of scale-invariant interactions to exactly 2ω [1, 2, 5, 6]. The main experimental platform for probing this symmetry and its breaking is the two-dimensional Fermi gas. Introducing the two-dimensional scattering length a_{2D} breaks classical scale invariance upon quantization—the quantum anomaly—and shifts the breathing frequency away from 2ω [3, 4, 7–9]. In realistic traps, weak anharmonicity and residual anisotropy further modify the response [10]. Experimentally, the near- 2ω mode and its anomalous shift have been measured in several ⁶Li experiments in quasi-two-dimensional geometries, with fractional shifts $|\delta\omega|/(2\omega) \sim 1\text{--}5\%$ [11–14].

On the theory side, the standard approach uses sum-rule [15, 16] or hydrodynamic [17, 18] methods, which express the breathing frequency (more precisely, a sum-rule centroid) in terms of the Tan contact and its derivatives [3, 4, 19]. Numerical studies of the breathing mode across the BCS–BEC crossover [20, 21] and exact analyses of mesoscopic conformal towers [22] provide complementary perspectives. All these treatments yield a single number—the centroid for the ground state or for the thermal ensemble—and do not resolve the radial structure within individual hyperangular channels of the trapped system.

In this paper we work within a single hyperangular channel and apply a classical identity for products of associated Laguerre polynomials [23, 24] to obtain closed-form matrix elements of the $1/R^2$ -weighted radial operator defined in Sec. II. The results hold for any real channel

parameter $s > 0$; we use two-dimensional notation and experimental context in the main text. The identity has three exact consequences:

1. *Exact solvability.* The $1/R^2$ perturbation is absorbed exactly into a shift of the channel parameter, $s \rightarrow s_\eta = \sqrt{s^2 + 2\eta\lambda_s/(\hbar\omega)}$ [25]. The model remains a harmonic oscillator with a shifted inverse-square term: radial gaps stay at $2\hbar\omega$ exactly, R^2 is tridiagonal in the exact eigenbasis, and no monopole spectral weight appears at forbidden frequencies at any order.
2. *Independent first-order algebraic proof.* The first-order cancellation of forbidden $\Delta q \neq \pm 1$ spectral weight is also proved by a compact perturbative argument in which the ket and bra contributions cancel pairwise, with the q - and s -dependence dropping out of each pair. This provides an independent verification and reveals structural detail that the exact-solvability argument alone does not display. We confirm it by exact diagonalization (Fig. 2). This is, to our knowledge, the main new result of this paper.
3. *Channel-resolved sum-rule estimate.* Substituting the exact single-channel quantities—the q -independent contact and the diagonal $\langle R^2 \rangle_{s,q} = a_{\text{ho}}^2 Q$ —into the m_1/m_{-1} sum-rule bound of Gao and Yu [19] yields a sum-rule estimate with Q^{-1} scaling ($Q \equiv 2q + s + 1$) and an explicit coefficient. Its finite-temperature average has a low- T plateau and a $1/T$ high- T tail.

The exact solvability and the algebraic cancellation proof are rigorous within the single-channel model for the operator \hat{C} defined in Sec. II. The sum-rule estimate is derived by substituting single-channel quantities into the many-body sum-rule framework [3, 4, 19]; the identification of the contact C_s with the model-operator value is

* tierz@simis.cn

exact for the two-body problem and is an approximation for $N > 2$ [26]. For $N > 2$ particles the single-channel results provide contributions from individual channels for the many-body breathing response. We discuss the behavior of these results under weak trap anisotropy, the distinction between the single-channel spectrum and the many-body mode frequency, and the connection to experiment via a single-point calibration of the channel coefficient κ_s .

The paper is organized as follows. Section II introduces the model, the notation, and the physical quantities we compute. Section III presents the Laguerre overlap identity and its proof. Section IV derives the closed matrix elements of \hat{C} and the q -independence of the diagonal element. Section V proves the exact solvability of the single-channel model and derives the sum-rule centroid for the channel. Section VI proves the exact vanishing of first-order spectral weight transfer, with an explicit worked example, a compact analytic cancellation formula, and numerical validation. Section VII gives the finite-temperature average of the sum-rule centroid. Sections VIII and IX discuss the effect of weak anisotropy and the experimental calibration procedure. Section X summarizes, discusses the three-dimensional extension and weak quartic anharmonicity, and presents an outlook.

II. MODEL, NOTATION, AND SCOPE

We work within a single hyperangular channel of the trapped two-body (or few-body) problem in an isotropic harmonic potential. In any spatial dimension d , the center-of-mass frame separates the relative motion into a hyperradial coordinate R and hyperangular coordinates Ω . The hyperangular part determines the channel index $s > 0$; in two dimensions s takes integer values related to the relative angular momentum, while in three dimensions it is typically half-integer or determined by the partial-wave structure [2, 25]. The hyperradial part is governed by an effective one-dimensional Schrödinger equation whose eigenstates are labeled by a radial quantum number $q = 0, 1, 2, \dots$

All exact single-channel results in this paper—the Laguerre overlap identity (Sec. III), the q -independent diagonal matrix element (Sec. IV), the exact solvability of the single-channel model (Sec. V C), and the preservation of the radial selection rule (Sec. VI)—hold for any real $s > 0$ and are therefore independent of the spatial dimension. The sum-rule centroid for the channel (Sec. V D) and its finite- T average (Sec. VII) are derived by inserting exact single-channel quantities into the sum-rule bound of Gao and Yu; their physical interpretation depends on the dimension and on the identification of \hat{C} with the physical contact (Sec. II). The dimension enters through the physical interpretation: which values of s are realized, the form of the anomaly parameter η , and the connection to experiment. The main text uses two-dimensional no-

tation and experimental context; the three-dimensional case is discussed in Sec. X.

The key quantum numbers and parameters appearing throughout the paper are collected in Table I for reference.

The hyperradial eigenfunctions within channel s are [25]

$$F_{s,q}(R) = \mathcal{N}_{s,q} R^{s+\frac{1}{2}} e^{-R^2/(2a_{\text{ho}}^2)} L_q^{(s)}(R^2/a_{\text{ho}}^2), \quad (1)$$

where $\mathcal{N}_{s,q}$ is a normalization constant and $L_q^{(s)}$ is the associated Laguerre polynomial of degree q and order s . The corresponding energies are

$$E_{s,q} = \hbar\omega (2q + s + 1) \equiv \hbar\omega Q. \quad (2)$$

The energy spacing between adjacent radial levels is exactly $2\hbar\omega$, independent of q . This uniform spacing is a hallmark of the harmonic oscillator and is intimately connected to the $SO(2,1)$ dynamical symmetry [1, 2, 6].

The quantum anomaly enters as a small perturbation to the Hamiltonian,

$$H = H_0 + \eta \hat{C},$$

where H_0 is the unperturbed (scale-invariant) Hamiltonian, \hat{C} is the single-channel $1/R^2$ -weighted operator defined below, and η is a dimensionless coupling that controls the strength of the scale-breaking.

TABLE I. Notation and definitions used throughout the paper.

Symbol	Definition
$s > 0$	hyperangular channel index
$q = 0, 1, 2, \dots$	radial quantum number
$Q \equiv 2q + s + 1$	dimensionless energy (in units of $\hbar\omega$)
$E_{s,q} = \hbar\omega Q$	unperturbed energy
$L_q^{(s)}(u)$	associated Laguerre polynomial
λ_s	channel normalization (Tan contact for $N=2$)
\hat{C}	$1/R^2$ -weighted single-channel operator ($\langle \hat{C} \rangle_{s,q} = \lambda_s/s$)
η	anomaly parameter
$\varepsilon_A^{(s)} \equiv \eta \lambda_s / (\hbar\omega)$	dimensionless anomaly strength (channel-dependent)
$\varepsilon_C^{(s)} \equiv E''(y) / (\hbar\omega)$	dimensionless energy curvature (channel-dependent)
κ_s	centroid coefficient for channel s ; Eq. (29)
y	logarithmic scale variable (in 2D: $\ln(a_{2D}/a_{\text{ref}})$)
$x \equiv e^{-2\hbar\omega/(k_B T)}$	Boltzmann factor per level
$T_{\text{ho}} \equiv \hbar\omega/k_B$	trap temperature scale
$a_{\text{ho}} \equiv \sqrt{\hbar/(m\omega)}$	harmonic oscillator length
$U_{s,q}$	$(q+1)(q+s+1)$; upward strength
$D_{s,q}$	$q(q+s)$; downward strength
$W_{s,q}$	$U_{s,q} + D_{s,q}$; total strength

Within the single channel at fixed s , the operator $\hat{\mathcal{C}}$ acts on the hyperradial degree of freedom. We *define* $\hat{\mathcal{C}}$ as the operator whose matrix elements in the hyperradial basis are proportional to the $1/R^2$ -weighted overlaps,

$$\langle s, q' | \hat{\mathcal{C}} | s, q \rangle \propto \int_0^\infty dR F_{s,q'}(R) \frac{1}{R^2} F_{s,q}(R),$$

with the overall normalization fixed by the Tan contact λ_s for the channel: $\langle s, q | \hat{\mathcal{C}} | s, q \rangle = \lambda_s/s$ (derived in Sec. IV). This normalization convention matches the adiabatic Tan relations [27–29], operator product expansion (OPE) treatments of the spectral response [30], and the general relations of Werner and Castin [26].

Physical identification. For the two-body problem in a harmonic trap, the short-distance behavior $F_{s,q}(R) \propto R^{s+1/2}$ as $R \rightarrow 0$ is governed entirely by the channel index s , and the $1/R^2$ weight in the matrix element is precisely the short-distance enhancement that enters the Tan contact [27, 30]; in this case $\hat{\mathcal{C}}$ coincides with the physical contact operator. Concretely, the two-body Tan adiabatic relation $\langle \hat{\mathcal{C}} \rangle = (m/2\pi) \partial E / \partial y$ [19, 27] and the energy $E_{s,q}(\eta) = \hbar\omega(2q + s_\eta + 1)$ from Sec. VC give $\langle \hat{\mathcal{C}} \rangle_{s,q} = (m/2\pi) \partial_y [\eta(y) \lambda_s(y) / s]$, which is q -independent and consistent with Eq. (10). For $N > 2$ particles, the projection of the physical Tan contact onto a single hyperangular channel may introduce additional structure (e.g., dependence on the many-body regular part [26]); the identification of $\hat{\mathcal{C}}$ with the physical contact then becomes an approximation whose accuracy depends on the separation of hyperradial and hyperangular degrees of freedom. All results in Secs. III–VI hold rigorously for $\hat{\mathcal{C}}$ as defined above; the physical interpretation requires the identification discussed here.

The energy curvature $E''(y) \equiv \partial^2 E / \partial y^2$ is taken with respect to the logarithmic scale variable y (in 2D, $y = \ln(a_{2D}/a_{\text{ref}})$; in 3D, y is the analogous renormalization variable). We combine the anomaly and curvature into dimensionless parameters $\varepsilon_A \equiv \eta \lambda_s / (\hbar\omega)$ and $\varepsilon_C \equiv E''(y) / (\hbar\omega)$. Both ε_A and ε_C depend on the channel s (through λ_s and the channel-specific energy curvature); we suppress the superscript (s) when the channel is clear from context.

a. Scope and applicability. Our results concern the *radial excitation spectrum within a single hyperangular channel*. The exact single-channel results (Secs. III–VI) and the exact solvability (Sec. VC) are rigorous at fixed s for the operator $\hat{\mathcal{C}}$ defined above; they hold for any $s > 0$. The physical identification of $\hat{\mathcal{C}}$ with the Tan contact is exact for the two-body problem, where the hyperradial channel *is* the full problem. Even for $N = 2$, the sum-rule centroid derived in Sec. VD is a sum-rule estimate, not the exact breathing frequency; exact two-body solutions [31] give a nontrivial scattering-length-dependent frequency. For $N > 2$ particles, the many-body breathing mode is a collective excitation involving all occupied channels and the full N -body density matrix; connecting our single-channel results to that mode requires an

additional step—summation over channels weighted by their many-body occupation—that we do not perform here. (For $N \geq 4$ fermions in 3D, the relevant values of the hyperangular parameter are not generally known in closed form [25], though the exact results hold for any $s > 0$.) We also do not address inter-channel coupling, strong-coupling effects, or finite effective range corrections beyond noting that the latter can be absorbed into the channel parameters λ_s and ε_C by calibration [32, 33].

III. THE LAGUERRE OVERLAP IDENTITY

The central analytical tool of this paper is a closed-form evaluation of the integral

$$J_{q,q'}^{(s)} \equiv \int_0^\infty du u^{s-1} e^{-u} L_q^{(s)}(u) L_{q'}^{(s)}(u). \quad (3)$$

This integral arises naturally as the matrix element of $\hat{\mathcal{C}}$ defined in Sec. II: the weight $u^{s-1} e^{-u}$ differs from the standard orthogonality weight $u^s e^{-u}$ by a factor of $1/u = a_{\text{ho}}^2/R^2$, which is the $1/R^2$ weight that defines the single-channel operator. For the two-body problem, this weight coincides with the short-distance enhancement associated with the physical Tan contact [27, 30]; for the general case, see the discussion in Sec. II.

a. Statement. For $s > 0$ and $q, q' \in \mathbb{N}_0$, let $m \equiv \min\{q, q'\}$. Then [23, 24]

$$J_{q,q'}^{(s)} = \Gamma(s) \frac{(s+1)_m}{m!} = \frac{\Gamma(s+m+1)}{s \Gamma(m+1)}, \quad (4)$$

where $(a)_m = a(a+1)\cdots(a+m-1) = \Gamma(a+m)/\Gamma(a)$ is the Pochhammer symbol. Equivalently, $J_{q,q'}^{(s)} = \Gamma(s) \binom{s+m}{m}$, with the binomial coefficient understood in its gamma-function generalization.

The crucial feature is that the integral depends only on $\min\{q, q'\}$, not on $\max\{q, q'\}$. In particular, $J_{0,q'}^{(s)} = \Gamma(s)$ for all q' : the overlap of any state with the ground state is a universal constant independent of the excited-state index.

b. Proof. We use the generating function for associated Laguerre polynomials [34],

$$\sum_{n \geq 0} L_n^{(s)}(u) t^n = (1-t)^{-s-1} \exp\left[-\frac{ut}{1-t}\right].$$

Multiplying two such generating functions (with parameters t and t') against the weight $u^{s-1} e^{-u}$ and integrating over u from 0 to ∞ gives

$$\begin{aligned} \sum_{q,q' \geq 0} J_{q,q'}^{(s)} t^q t'^{q'} &= \int_0^\infty du u^{s-1} e^{-u} \frac{e^{-ut/(1-t)}}{(1-t)^{s+1}} \frac{e^{-ut'/(1-t')}}{(1-t')^{s+1}} \\ &= \frac{\Gamma(s)}{(1-t)(1-t')} (1-tt')^{-s}. \end{aligned} \quad (5)$$

The last step uses the fact that the three exponentials combine into $e^{-u/[(1-t)(1-t')/(1-tt')]}$, and the resulting Euler gamma integral evaluates to $\Gamma(s)$ times a rational function of t and t' .

Now expand $(1 - tt')^{-s}$ using the binomial series:

$$(1 - tt')^{-s} = \sum_{m \geq 0} \frac{\binom{s}{m}}{m!} (tt')^m.$$

Together with the factor $1/[(1-t)(1-t')] = \sum_{a \geq 0} t^a \cdot \sum_{b \geq 0} t'^b$, the product generates terms $t^q t'^{q'}$ with $q \geq m$ and $q' \geq m$. Matching the coefficient of $t^q t'^{q'}$ gives

$$J_{q,q'}^{(s)} = \Gamma(s) \sum_{k=0}^{\min\{q,q'\}} \frac{\binom{s}{k}}{k!},$$

which reduces to (4) by the ‘‘telescoping’’ identity for Pochhammer symbols: $\sum_{k=0}^m \binom{s}{k}/k! = (s+1)_m/m!$. \square

c. Numerical verification. The identity (4) has been verified by numerical quadrature against the integral definition (3) for $s = 1, 2, 3, 4$ and all pairs (q, q') with $q, q' = 0, \dots, 9$. The agreement is to machine precision ($\sim 10^{-15}$).

IV. CLOSED CONTACT MATRIX ELEMENTS

We now apply the identity to compute the matrix elements of $\hat{\mathcal{C}}$. Define

$$I_\alpha(q) \equiv \int_0^\infty du u^\alpha e^{-u} [L_q^{(s)}(u)]^2. \quad (6)$$

The normalization integral for the hyperradial eigenstates is $I_s(q) = \Gamma(q+s+1)/\Gamma(q+1)$ (a standard Laguerre result [34]), and the diagonal contact matrix element is proportional to $I_{s-1}(q)$.

a. The contact ratio. A direct consequence of (4) is

$$\frac{I_{s-1}(q)}{I_s(q)} = \frac{1}{s} \quad \text{for all } q \geq 0. \quad (7)$$

Proof. Note that $I_{s-1}(q) = J_{q,q}^{(s)}$ (set $q' = q$ in (3)), which equals $\Gamma(s)(s+1)_q/q!$ by (4). For $q = 0$, the claim is immediate since $I_{s-1}(0) = \Gamma(s)$ and $I_s(0) = \Gamma(s+1) = s\Gamma(s)$.

For $q \geq 1$, $I_s(q)$ is obtained by inserting an extra factor of u via the Laguerre recurrence relation [23, 34]:

$$u L_q^{(s)}(u) = (2q + s + 1) L_q^{(s)}(u) - (q + 1) L_{q+1}^{(s)}(u) - (q + s) L_{q-1}^{(s)}(u). \quad (8)$$

Inserting this into $I_s(q) = \int_0^\infty u \cdot u^{s-1} e^{-u} [L_q^{(s)}]^2 du$ and using the fact that one factor of $L_q^{(s)}$ is untouched while

the other is expanded via (8), we get three integrals—all of the form $J_{q,q'}^{(s)}$ for different values of q' :

$$\begin{aligned} I_s(q) &= (2q+s+1) J_{q,q}^{(s)} - (q+1) J_{q,q+1}^{(s)} \\ &\quad - (q+s) J_{q,q-1}^{(s)} \\ &= (2q+s+1) J_{q,q}^{(s)} - (q+1) J_{q,q+1}^{(s)} \\ &\quad - (q+s) J_{q-1,q}^{(s)}, \end{aligned} \quad (9)$$

where we used $J_{q,q-1}^{(s)} = J_{q-1,q}^{(s)}$ (symmetry of (3)).

Now apply (4). Since $\min\{q, q\} = q$, $\min\{q, q+1\} = q$, and $\min\{q-1, q\} = q-1$:

$$\begin{aligned} J_{q,q}^{(s)} &= \Gamma(s) \frac{(s+1)_q}{q!}, \\ J_{q,q+1}^{(s)} &= \Gamma(s) \frac{(s+1)_q}{q!} \quad (\text{same! min is still } q), \\ J_{q-1,q}^{(s)} &= \Gamma(s) \frac{(s+1)_{q-1}}{(q-1)!}. \end{aligned}$$

Substituting and simplifying (using $(s+1)_q/q! = (s+1)_{q-1}/(q-1)! \cdot (s+q)/q$):

$$\begin{aligned} I_s(q) &= \Gamma(s) \frac{(s+1)_q}{q!} [(2q+s+1) - (q+1)] \\ &\quad - (q+s) \Gamma(s) \frac{(s+1)_{q-1}}{(q-1)!} \\ &= (q+s) \Gamma(s) \left[\frac{(s+1)_q}{q!} - \frac{(s+1)_{q-1}}{(q-1)!} \right] \\ &= (q+s) \Gamma(s) \frac{(s+1)_{q-1}}{(q-1)!} \left[\frac{s+q}{q} - 1 \right] \\ &= s \Gamma(s) \frac{(s+1)_q}{q!} = s I_{s-1}(q). \end{aligned}$$

Hence $I_{s-1}(q)/I_s(q) = 1/s$. \square

b. Physical meaning. The ratio (7) tells us that

$$\langle s, q | \hat{\mathcal{C}} | s, q \rangle = \frac{\lambda_s}{s} \quad \text{for all } q \geq 0. \quad (10)$$

That is, the diagonal matrix element of the single-channel operator $\hat{\mathcal{C}}$ is the same in every radial eigenstate within a given channel. The ground state ($q = 0$) and all excited states ($q = 1, 2, \dots$) yield the same value. This can be understood physically: the short-distance behavior of the hyperradial wavefunction, $F_{s,q}(R) \propto R^{s+1/2}$ as $R \rightarrow 0$, is controlled entirely by the channel index s ; changing q only adds nodes at $R \sim a_{\text{ho}}$ without affecting the short-distance boundary condition. Since the $1/R^2$ weight in $\hat{\mathcal{C}}$ probes precisely this short-distance structure, the matrix element depends on s but not on the radial quantum number q . Equation (7) makes this intuition exact in the harmonic basis. For the two-body problem, where $\hat{\mathcal{C}}$ coincides with the physical Tan contact (Sec. II), this establishes q -independence of the physical contact within the channel.

This result is verified numerically: $I_{s-1}(q)/I_s(q)$ agrees with $1/s$ to machine precision for $s = 1, 2, 3, 4$ and $q = 0, \dots, 9$.

V. EXACT SOLVABILITY, MONOPOLE MOMENTS, AND SUM-RULE CENTROID

We now compute the single-channel monopole moments, prove the exact solvability of the single-channel model, and derive the channel-resolved sum-rule centroid.

A. The R^2 operator and its tridiagonality

The breathing mode is driven by the operator $F = R^2$, the squared hyperradius. Using the Laguerre recurrence (8), the matrix elements of R^2 in the orthonormal hyperradial basis $\{|s, q\rangle\}$ are

$$\begin{aligned} \langle s, q' | R^2 | s, q \rangle &= a_{\text{ho}}^2 \left[Q \delta_{q', q} \right. \\ &\quad \left. - \sqrt{(q+1)(q+s+1)} \delta_{q', q+1} - \sqrt{q(q+s)} \delta_{q', q-1} \right], \end{aligned} \quad (11)$$

with $Q = 2q + s + 1$. That is, R^2 is *tridiagonal* in the radial index q : it connects each level only to its nearest neighbors $q \pm 1$. This three-term structure is the radial manifestation of the $SO(2, 1)$ algebra of the isotropic harmonic oscillator. In the scale-invariant limit it enforces the undamped monopole mode at exactly 2ω [1, 2].

B. Sum-rule moments

In the standard many-body sum-rule approach [15, 16, 35], one computes moments of the dynamic structure factor for the many-body ground state. Here we consider a simpler object: the moments of the single-state, two-sided spectrum of R^2 from a prepared eigenstate $|s, q\rangle$. This is not the standard collective-mode construction, but it serves to establish notation and to demonstrate the role of the signed energy differences.

Starting from level $|i\rangle = |s, q\rangle$, the energy-weighted and inverse-energy-weighted moments are

$$m_1 \equiv \sum_f (E_f - E_i) |\langle f | R^2 | i \rangle|^2, \quad (12)$$

$$m_{-1} \equiv \sum_f \frac{|\langle f | R^2 | i \rangle|^2}{E_f - E_i}. \quad (13)$$

Because R^2 is tridiagonal, only $f = q \pm 1$ contribute. The energy gaps are $E_{q+1} - E_q = +2\hbar\omega$ and $E_{q-1} - E_q = -2\hbar\omega$, and the squared matrix elements are $|\langle q+1 | R^2 | q \rangle|^2 = a_{\text{ho}}^4 (q+1)(q+s+1)$ and $|\langle q-1 | R^2 | q \rangle|^2 = a_{\text{ho}}^4 q(q+s)$.

Because the energy differences in (12) and (13) carry a sign, the upward and downward contributions partially cancel. Specifically:

$$m_1 = 2\hbar\omega a_{\text{ho}}^4 [(q+1)(q+s+1) - q(q+s)] = 2\hbar\omega a_{\text{ho}}^4 Q, \quad (14)$$

$$m_{-1} = \frac{a_{\text{ho}}^4}{2\hbar\omega} [(q+1)(q+s+1) - q(q+s)] = \frac{a_{\text{ho}}^4}{2\hbar\omega} Q, \quad (15)$$

where we used $(q+1)(q+s+1) - q(q+s) = 2q + s + 1 = Q$. The sum-rule centroid is

$$\omega_B^2 \equiv \frac{m_1}{m_{-1}} = (2\omega)^2 \quad (16)$$

in the unperturbed (scale-invariant) system, independent of q , confirming the $SO(2, 1)$ prediction.

Remark: upward, downward, and total strengths. It is useful to name the individual squared matrix elements:

$$U_{s,q} \equiv (q+1)(q+s+1), \quad D_{s,q} \equiv q(q+s). \quad (17)$$

Here $U_{s,q} = |\langle q+1 | R^2 | q \rangle|^2 / a_{\text{ho}}^4$ is the upward (absorption) strength and $D_{s,q} = |\langle q-1 | R^2 | q \rangle|^2 / a_{\text{ho}}^4$ is the downward (emission) strength. Note that $D_{s,q+1} = (q+1)(q+s+1) = U_{s,q}$: the downward strength from level $q+1$ is the same as the upward strength from level q , as it must be since both refer to the same physical transition. The signed moments involve the difference,

$$Q = U_{s,q} - D_{s,q} = 2q + s + 1,$$

while the total unsigned oscillator strength is the sum,

$$W_{s,q} \equiv U_{s,q} + D_{s,q} = (q+1)(q+s+1) + q(q+s). \quad (18)$$

In the standard positive-frequency thermal response, the natural weight for the $q \rightarrow q+1$ transition is $U_{s,q}$, not $W_{s,q}$ (see Sec. VII).

C. Exact solvability of the single-channel model

The eigenfunctions (1) satisfy the radial Schrödinger equation for the Hamiltonian [2, 25]

$$H_{0,s} = \frac{\hbar\omega}{2} \left[-\frac{d^2}{d\rho^2} + \rho^2 + \frac{s^2 - \frac{1}{4}}{\rho^2} \right], \quad \rho \equiv R/a_{\text{ho}}, \quad (19)$$

with eigenvalues $E_{s,q} = \hbar\omega(2q+s+1)$. The single-channel perturbation $\eta\hat{C} = \eta\lambda_s a_{\text{ho}}^2 / R^2 = \eta\lambda_s / \rho^2$ adds an inverse-square term to the centrifugal barrier, so the full single-channel Hamiltonian is

$$H_{s,\eta} = \frac{\hbar\omega}{2} \left[-\frac{d^2}{d\rho^2} + \rho^2 + \frac{s_\eta^2 - \frac{1}{4}}{\rho^2} \right], \quad (20)$$

where

$$s_\eta \equiv \sqrt{s^2 + \frac{2\eta\lambda_s}{\hbar\omega}}. \quad (21)$$

The perturbed Hamiltonian is therefore a harmonic oscillator with the shifted parameter s_η in place of s . Its exact eigenstates and spectrum are [25]

$$F_{s_\eta, q}(R) = \mathcal{N}_{s_\eta, q} R^{s_\eta + \frac{1}{2}} e^{-R^2/(2a_{\text{ho}}^2)} L_q^{(s_\eta)}(R^2/a_{\text{ho}}^2), \quad (22)$$

$$E_{s_\eta, q}(\eta) = \hbar\omega (2q + s_\eta + 1). \quad (23)$$

Three exact consequences follow.

First, the energy gaps are

$$E_{s, q+1}(\eta) - E_{s, q}(\eta) = 2\hbar\omega \quad \text{exactly, at all orders in } \eta. \quad (24)$$

Second, since the exact eigenstates (22) are Laguerre functions (with parameter s_η), the operator R^2 is tridiagonal in the exact eigenbasis by the standard three-term Laguerre recurrence [34]. There is therefore no monopole spectral weight at forbidden frequencies $\pm 4\omega$, $\pm 6\omega$, ... at *any* order in η , not only at first order.

Third, expanding (21) for small η ,

$$s_\eta = s + \frac{\eta\lambda_s}{\hbar\omega s} + O(\eta^2),$$

so the first-order energy shift is $\eta\lambda_s/s$, independent of q , reproducing Eq. (10).

The single-channel monopole response therefore satisfies

$$\omega_{s, q \rightarrow q+1} = 2\omega \quad \text{exactly for all } \eta, \quad (25)$$

within the single-channel model. Physically, the $1/R^2$ operator is homogeneous of degree -2 in R and therefore scale-invariant [1, 2]; adding it to H_0 shifts the centrifugal strength (the $SO(2, 1)$ Casimir eigenvalue) from $s^2 - \frac{1}{4}$ to $s_\eta^2 - \frac{1}{4}$ but preserves the dynamical symmetry, so the breathing frequency remains pinned to 2ω [9].

a. Relation to the perturbative proof. The first-order cancellation proved in Sec. VI is the perturbative manifestation of the exact all-order result above. The algebraic cancellation—in which the ket and bra contributions cancel pairwise, with the q - and s -dependence dropping out of each pair—provides an independent verification and reveals structural detail that the exact-solvability argument alone does not display.

D. Channel-resolved sum-rule centroid

The exact result (25) shows that the single-channel line does not shift. The physical breathing mode of the many-body trapped gas *does* shift; in the standard sum-rule approach [3, 4, 19] the sum-rule estimate is expressed through the m_1/m_{-1} ratio for the monopole operator in the many-body ground state. In the 2D framework of Gao and Yu [19], the m_1/m_{-1} upper bound [their Eqs. (21)–(22)] satisfies

$$\omega_{1, -1}^2 = \frac{(2\omega)^2}{1 - \Delta}, \quad \Delta = \frac{\pi(2 + \partial_y)C}{2m^2\omega^2 \langle \hat{O} \rangle}, \quad (26)$$

where $y = \ln a_{2D}$, C is the Tan contact [related to the energy by the adiabatic relation $C = (m/2\pi) \partial E / \partial y$, Gao and Yu, Eq. (8)], and $\langle \hat{O} \rangle = \langle R^2 \rangle$ for two particles.

We now substitute single-channel quantities into the sum rule. Within channel s at radial level q , the exact diagonal matrix element of R^2 is $\langle R^2 \rangle_{s, q} = a_{\text{ho}}^2 Q$ from Eq. (11), and the q -independence of the diagonal matrix element (Eq. (10)) implies that the contact $C_s(y)$ within the channel is q -independent. Substituting,

$$\Delta_{s, q} = \frac{\pi(2 + \partial_y)C_s}{2m^2\omega^2 a_{\text{ho}}^2 Q}. \quad (27)$$

Linearizing $\omega_{1, -1} \approx 2\omega(1 + \Delta/2)$ for small symmetry breaking gives

$$\frac{\delta\omega_{s, q}^{\text{SR}}}{2\omega} = \frac{\kappa_s}{2Q} + O(\kappa_s^2), \quad Q \equiv 2q + s + 1, \quad (28)$$

where the centroid coefficient for channel s is now a *derived* quantity:

$$\kappa_s \equiv \frac{\pi(2 + \partial_y)C_s}{2m^2\omega^2 a_{\text{ho}}^2}. \quad (29)$$

The Q^{-1} scaling follows from the interplay of two exact results: the q -independent contact C_s (from the Laguerre identity) and the Q -proportional expectation value of R^2 (from the Laguerre recurrence). If one identifies C_s with the model-operator value, $C_s = \lambda_s/s$, then κ_s reduces to a combination of λ_s , its scale derivative, and the channel parameter s . For the two-body problem, where \hat{C} coincides with the physical contact (Sec. II), this identification is exact. For $N > 2$, κ_s should be treated as a single empirical parameter absorbing contributions not resolved by the single-channel analysis [26].

At $q = 0$ the formula matches the standard sum-rule structure [3, 4, 19]; for $q > 0$ it resolves the estimate level by level, predicting a monotone suppression with the Q^{-1} scaling (Fig. 1a).

a. Exact line versus sum-rule centroid. Within the single channel, Eq. (25) guarantees that the spectral function remains a delta function at 2ω exactly: the single-channel line is *sharp* and *unshifted*. The sum-rule estimate (28) describes a shifted frequency because the sum-rule bound of Gao and Yu incorporates the scale dependence of the energy (the Tan adiabatic relation [27]) and the equation of state, contributions not visible in the single-channel spectrum. For $N > 2$, extracting the observed frequency requires the inter-channel summation discussed in Sec. X.

b. Large- q behavior. Since $Q = 2q + s + 1$:

$$\frac{\delta\omega_{s, q}^{\text{SR}}}{2\omega} = \frac{\kappa_s}{4q} + O(q^{-2}).$$

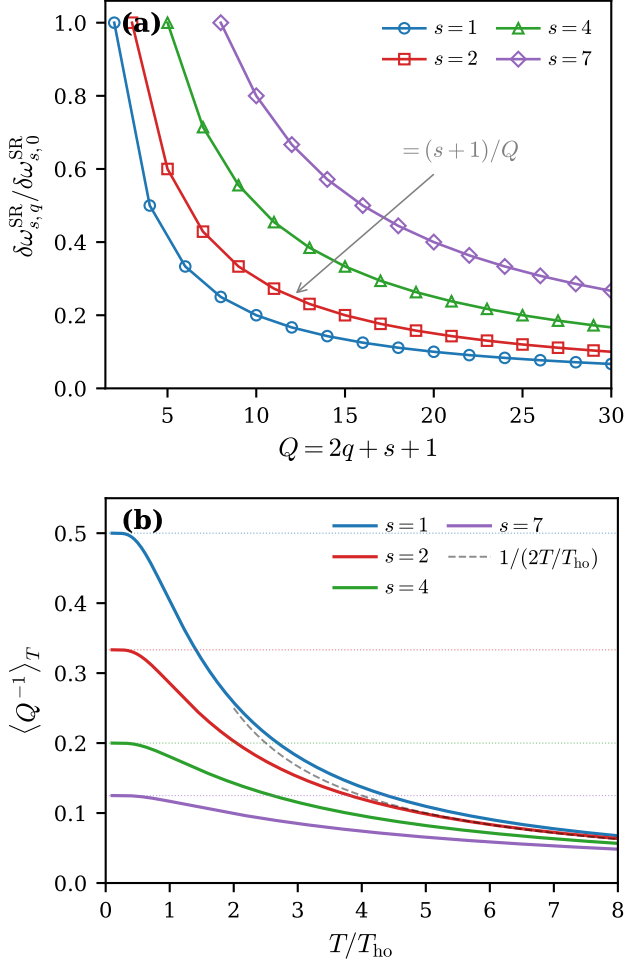


FIG. 1. (a) Sum-rule centroid normalized to its value at $q = 0$: $\delta\omega_{s,q}^{\text{SR}}/\delta\omega_{s,0}^{\text{SR}} = (s+1)/Q$, with $Q \equiv 2q + s + 1$. This shows the parameter-free Q^{-1} suppression of higher radial levels after a single-point calibration of κ_s . (b) Thermal average $\langle Q^{-1} \rangle_T$ weighted by the upward strength $U_{s,q}$, showing the low- T plateau $(s+1)^{-1}$ and the universal high- T tail $1/(2T/T_{\text{ho}})$.

VI. FIRST-ORDER SPECTRAL WEIGHT TRANSFER VANISHES

We now present the independent algebraic proof of the first-order spectral-weight cancellation announced in Sec. V C. While the exact solvability of the single-channel model (Sec. V C) already implies that no spectral weight is transferred at any order, the perturbative cancellation mechanism is of independent interest: the ket and bra contributions cancel pairwise, with the q - and s -dependence dropping out of each pair, revealing algebraic structure that the exact-solvability argument alone does not display. The analogous question in the many-body context—whether the contact perturbation broadens the breathing line—is directly relevant to the interpretation of spectral measurements [11, 12].

A. Setup

In the unperturbed system, the operator R^2 connects level q only to $q \pm 1$ (tridiagonality). This means the monopole spectral function, viewed from any level q , has all its weight at frequencies $\pm 2\omega$: upward transitions $q \rightarrow q+1$ at $+2\omega$ and (for $q \geq 1$) downward transitions $q \rightarrow q-1$ at -2ω . There is no weight at $\pm 4\omega, \pm 6\omega$, etc. When the anomaly is turned on, the eigenstates are perturbed: $|\tilde{q}\rangle = |q\rangle + O(\eta)$. The question is whether the perturbed matrix element $\langle \tilde{q} + 2 | R^2 | \tilde{q} \rangle$, which was zero at zeroth order, becomes nonzero at $O(\eta)$.

If it does, there is spectral weight at frequency $\approx 4\omega$ (the energy gap between levels q and $q+2$), and the breathing line would broaden. If it remains zero, the line stays sharp.

B. First-order perturbation theory

At first order in η , the perturbed states are

$$|\tilde{q}\rangle = |q\rangle + \eta \sum_{m \neq q} \frac{\langle m | \hat{C} | q \rangle}{E_q - E_m} |m\rangle, \quad (30)$$

$$\langle \tilde{q} + 2 | = \langle q + 2 | + \eta \sum_{n \neq q+2} \frac{\langle q + 2 | \hat{C} | n \rangle}{E_{q+2} - E_n} \langle n |. \quad (31)$$

The first-order correction to $\langle q + 2 | R^2 | q \rangle$ (which is zero at zeroth order) is

$$\begin{aligned} \langle \tilde{q} + 2 | R^2 | \tilde{q} \rangle^{(1)} &= \eta \left(\underbrace{\sum_{m \neq q} \frac{\langle q + 2 | R^2 | m \rangle \langle m | \hat{C} | q \rangle}{E_q - E_m}}_{\text{ket correction}} \right. \\ &\quad \left. + \underbrace{\sum_{n \neq q+2} \frac{\langle q + 2 | \hat{C} | n \rangle \langle n | R^2 | q \rangle}{E_{q+2} - E_n}}_{\text{bra correction}} \right). \end{aligned} \quad (32)$$

C. Off-diagonal contact matrix elements

To evaluate the perturbative sums, we need the off-diagonal elements of \hat{C} $\langle q' | \hat{C} | q \rangle$ with $q' > q$. These are related to contact matrix elements that also appear in OPE-based treatments of the spectral response [30]. From the identity (4), $J_{q',q}^{(s)}$ with $q' > q$ has $\min\{q', q\} = q$, so $J_{q',q}^{(s)} = \Gamma(s)(s+1)_q/q!$ (the same value as $J_{q,q}^{(s)}$, independent of how far above q' is). Dividing by the norms gives

$$\langle q + \Delta | \hat{C} | q \rangle = \frac{\lambda_s}{s} \prod_{j=1}^{\Delta} \sqrt{\frac{q+j}{q+s+j}}, \quad \Delta = 1, 2, 3, \dots \quad (33)$$

In particular, the elements needed below are:

$$\begin{aligned}\langle q+1|\hat{\mathcal{C}}|q\rangle &= \frac{\lambda_s}{s} \sqrt{\frac{q+1}{q+s+1}}, \\ \langle q+2|\hat{\mathcal{C}}|q\rangle &= \frac{\lambda_s}{s} \sqrt{\frac{(q+1)(q+2)}{(q+s+1)(q+s+2)}}, \\ \langle q+3|\hat{\mathcal{C}}|q\rangle &= \frac{\lambda_s}{s} \sqrt{\frac{(q+1)(q+2)(q+3)}{(q+s+1)(q+s+2)(q+s+3)}}.\end{aligned}$$

Note the pattern: each factor $\sqrt{(q+j)/(q+s+j)}$ is less than 1 for $s > 0$, so the off-diagonal elements decrease with $|\Delta|$.

D. Identifying the contributing terms

Because R^2 is tridiagonal, $\langle q+2|R^2|m\rangle$ is nonzero only for $m \in \{q+1, q+2, q+3\}$. Combined with the constraint $m \neq q$ (which is automatically satisfied for these values), the ket correction has exactly three terms.

Similarly, $\langle n|R^2|q\rangle$ is nonzero only for $n \in \{q-1, q, q+1\}$, and the constraint $n \neq q+2$ is automatically satisfied. The bra correction has at most three terms (two if $q = 0$, since $n = q-1 = -1$ does not exist).

Inserting the R^2 matrix elements from (11), the contact elements from (33), and the energy denominators $E_q - E_m = -2(m-q)\hbar\omega$, each term takes the form $(a_{\text{ho}}^2 \lambda_s)/(s \cdot \hbar\omega)$ times a rational function of q and s .

E. Worked example: $s = 2, q = 0$

We demonstrate the cancellation explicitly for the simplest nontrivial case. With $s = 2$ and $q = 0$ (so $Q = 3$, final state $q_f = 2$), the relevant matrix elements are:

$$\begin{aligned}\langle 1|\hat{\mathcal{C}}|0\rangle &= \frac{\lambda_2}{2\sqrt{3}}, & \langle 2|R^2|1\rangle &= -2\sqrt{2} a_{\text{ho}}^2, \\ \langle 2|\hat{\mathcal{C}}|0\rangle &= \frac{\lambda_2}{2\sqrt{6}}, & \langle 2|R^2|2\rangle &= 7 a_{\text{ho}}^2, \\ \langle 3|\hat{\mathcal{C}}|0\rangle &= \frac{\lambda_2}{2\sqrt{10}}, & \langle 2|R^2|3\rangle &= -\sqrt{15} a_{\text{ho}}^2, \\ \langle 2|\hat{\mathcal{C}}|1\rangle &= \frac{\lambda_2}{2\sqrt{2}}, & \langle 0|R^2|0\rangle &= 3 a_{\text{ho}}^2, \\ & & \langle 1|R^2|0\rangle &= -\sqrt{3} a_{\text{ho}}^2.\end{aligned}$$

With the common prefactor $\mathcal{P} \equiv \lambda_2 a_{\text{ho}}^2/(4\sqrt{6} \hbar\omega)$ (note that η is already factored out in Eq. (32)), the five terms contributing to the bracket are:

$$\begin{aligned}\text{Ket } m=1: & \quad + 4 \mathcal{P}, \\ \text{Ket } m=2: & \quad - \frac{7}{2} \mathcal{P}, \\ \text{Ket } m=3: & \quad + 1 \mathcal{P}, \\ \text{Bra } n=0: & \quad + \frac{3}{2} \mathcal{P}, \\ \text{Bra } n=1: & \quad - 3 \mathcal{P}.\end{aligned}$$

The ket sum is $(4 - 7/2 + 1)\mathcal{P} = +3/2\mathcal{P}$ and the bra sum is $(3/2 - 3)\mathcal{P} = -3/2\mathcal{P}$, giving zero exactly. The term $n = q-1 = -1$ is absent at $q = 0$; for $q \geq 1$ there is a sixth term, and the cancellation still holds (verified for all s and q tested, see Sec. VIH).

F. General cancellation

The cancellation demonstrated above for $s = 2, q = 0$ persists for all $s > 0$ and $q \geq 0$:

$$\langle \tilde{q}+2|R^2|\tilde{q}\rangle^{(1)} = 0 \quad \text{for all } s > 0, q \geq 0. \quad (34)$$

The same argument applies to $\langle \tilde{q}-2|R^2|\tilde{q}\rangle$ (the downward $q \rightarrow q-2$ channel). *There is no transfer of spectral weight at first order in the anomaly.*

In fact, the general first-order amplitude can be summed in closed form. Factoring out

$$\mathcal{A}_{s,q} \equiv \frac{\eta \lambda_s a_{\text{ho}}^2}{s \hbar\omega} \sqrt{\frac{(q+1)(q+2)}{(q+s+1)(q+s+2)}},$$

the ket correction equals

$$\begin{aligned}\mathcal{A}_{s,q} \left[\frac{q+s+2}{2} - \frac{2q+s+5}{4} + \frac{q+3}{6} \right] \\ = \mathcal{A}_{s,q} \frac{2q+3s+3}{12},\end{aligned}$$

while the bra correction equals

$$\begin{aligned}\mathcal{A}_{s,q} \left[-\frac{q}{6} + \frac{2q+s+1}{4} - \frac{q+s+1}{2} \right] \\ = -\mathcal{A}_{s,q} \frac{2q+3s+3}{12}.\end{aligned}$$

(The $q = 0$ case is included automatically, since the $-q/6$ term vanishes.) The two pieces cancel exactly, making the result (34) fully analytic.

a. Extension to all $\ell \geq 2$. The same cancellation holds for every forbidden channel $q \rightarrow q + \ell$ with $\ell \geq 2$. We give the explicit derivation.

Because R^2 is tridiagonal, the first-order amplitude (32) receives three ket terms ($m = q+\ell-1, q+\ell, q+\ell+1$) and three bra terms ($n = q-1, q, q+1$). For $\ell \geq 2$ no exclusions $m \neq q$ or $n \neq q+\ell$ are needed. Factor out $\mathcal{P} \equiv \eta c_\ell(q) a_{\text{ho}}^2/(2\hbar\omega)$ with $c_\ell(q) \equiv \langle q+\ell|\hat{\mathcal{C}}|q\rangle$.

Ket terms. The energy denominators are $E_q - E_m = -2(m-q)\hbar\omega$. Each term involves a product of an R^2 element and a contact ratio $c_\delta(q)/c_\ell(q)$. Using Eq. (33), the contact ratios simplify via $c_{\ell-1}(q)/c_\ell(q) = \sqrt{(q+s+\ell)/(q+\ell)}$ and $c_{\ell+1}(q)/c_\ell(q) = \sqrt{(q+\ell+1)/(q+s+\ell+1)}$, so the products of R^2 elements and contact ratios collapse (using $\sqrt{a/b} \cdot \sqrt{ab} = a$):

$$(K1) \quad m=q+\ell-1: \quad \frac{-(q+s+\ell)}{-2(\ell-1)} = \frac{q+s+\ell}{2(\ell-1)},$$

$$(K2) \quad m=q+\ell: \quad \frac{Q+2\ell}{-2\ell} = -\frac{Q+2\ell}{2\ell},$$

$$(K3) \quad m=q+\ell+1: \quad \frac{-(q+\ell+1)}{-2(\ell+1)} = \frac{q+\ell+1}{2(\ell+1)}.$$

Bra terms. The energy denominators are $E_{q+\ell} - E_n = 2(q+\ell-n)\hbar\omega$. For the contact ratios with shifted base point, the same product pattern gives $c_{\ell+1}(q-1)/c_\ell(q) = \sqrt{q/(q+s)}$ and $c_{\ell-1}(q+1)/c_\ell(q) = \sqrt{(q+s+1)/(q+1)}$:

$$(B1) \quad n=q-1: \quad \frac{-q}{2(\ell+1)} = -\frac{q}{2(\ell+1)},$$

$$(B2) \quad n=q: \quad \frac{Q}{2\ell} = \frac{Q}{2\ell},$$

$$(B3) \quad n=q+1: \quad \frac{-(q+s+1)}{2(\ell-1)} = -\frac{q+s+1}{2(\ell-1)}.$$

The six terms pair naturally by energy denominator:

$$\text{pair } (\ell-1): \quad K1+B3 = \frac{(q+s+\ell)-(q+s+1)}{2(\ell-1)} = \frac{1}{2},$$

$$\text{pair } (\ell): \quad K2+B2 = \frac{-(Q+2\ell)+Q}{2\ell} = -1,$$

$$\text{pair } (\ell+1): \quad K3+B1 = \frac{(q+\ell+1)-q}{2(\ell+1)} = \frac{1}{2}.$$

Each pair collapses to a constant independent of q and s , and the total is $\frac{1}{2} - 1 + \frac{1}{2} = 0$. (At $q=0$ the $n=q-1$ term is absent, but so is the $-q/(2(\ell+1))$ contribution.) The downward channels $q \rightarrow q-\ell$ follow by the same argument. Thus

$$\langle \tilde{q}+\ell | R^2 | \tilde{q} \rangle^{(1)} = 0 \quad \text{for all } \ell \geq 2, s > 0, q \geq 0, \quad (35)$$

which is the full statement of selection-rule preservation: the contact perturbation transfers no monopole spectral weight away from $\pm 2\omega$ at first order.

Remark on normalization. The first-order kets used in (32) are not normalized. However, since $\langle \tilde{q} | \tilde{q} \rangle = 1 + O(\eta^2)$, the normalization correction enters only at $O(\eta^2)$; moreover, it multiplies the zeroth-order matrix element $\langle q+\ell | R^2 | q \rangle = 0$, so it cannot generate spectral weight at forbidden frequencies.

G. Physical interpretation

Why is spectral weight not redistributed? One ingredient is the q -independence of the diagonal contact, Eq. (10). Because $\langle \hat{C} \rangle_{s,q} = \lambda_s/s$ for all q , the contact perturbation shifts all levels in a channel by the same amount. A uniform level shift removes any first-order gap-shift mechanism within the channel.

The residue correction, however, is controlled by the *off-diagonal* contact elements $\langle q' | \hat{C} | q \rangle$ with $q' \neq q$. Their special structure (inherited from the gamma-ratio identity (4)) conspires with the tridiagonality of R^2 to produce exact cancellation between ket and bra corrections. The vanishing spectral weight transfer is therefore a consequence of both the uniform diagonal shift and the closed off-diagonal pattern.

The physical consequence is that the breathing line remains spectrally sharp: the exact solvability (Sec. VC) guarantees this at all orders, while the perturbative cancellation proved here confirms the mechanism at $O(\eta)$. The sum-rule centroid (28) describes a shifted frequency arising from the many-body equation of state, but the

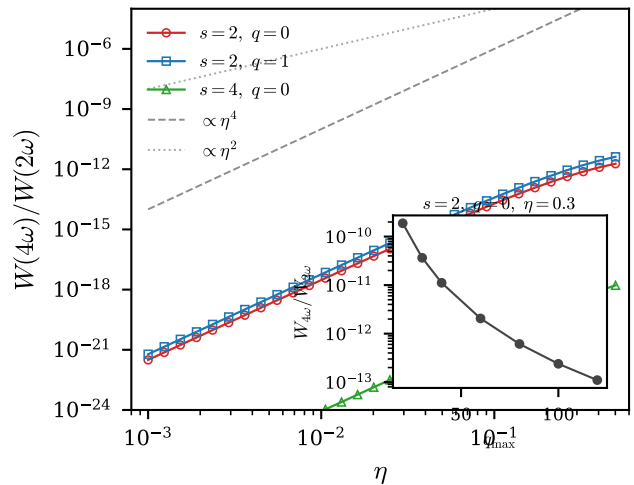


FIG. 2. Spectral weight at 4ω relative to the weight at 2ω , from exact diagonalization. The η^4 scaling (dashed line) confirms that the first-order transfer amplitude vanishes; the dotted line shows η^2 , the scaling that would obtain if spectral weight were redistributed at first order. Inset: basis-size dependence of the residual 4ω weight for $s=2$, $q=0$, $\eta=0.3$. The rapid decrease with q_{\max} confirms that the nonzero value in the truncated unperturbed basis is a numerical artifact; in the exact single-channel model with shifted parameter s_η the forbidden weight vanishes identically (Sec. VC).

single-channel line itself does not broaden or shift. This is consistent with both the theoretical expectation [36, 37] and the experimental observation that the breathing mode remains a well-defined, narrow spectral feature even in the presence of measurable anomalous shifts [11–14].

H. Numerical validation

a. First-order perturbation theory. We evaluate the ket and bra sums in (32) numerically using the analytic matrix elements of \hat{C} from (4). For all tested values of s and q ($s=1, 2, 4$; $q=0, 1, 2, 5, 10$), the ket and bra sums cancel to machine precision, with residuals $\lesssim 10^{-15}$.

b. Exact diagonalization. We construct the full Hamiltonian $H = H_0 + \eta\hat{C}$ as a matrix in the truncated basis $\{|s, q\rangle : q=0, \dots, q_{\max}\}$ with $q_{\max}=80$, diagonalize it, and compute the R^2 spectral function from each eigenstate. Figure 2 shows the spectral weight at frequency 4ω (the $q \rightarrow q+2$ channel), normalized by the weight at 2ω , as a function of η for several values of (s, q) .

The η^4 scaling at small η is the key signature: since the spectral weight is $|\langle \tilde{q}+2 | R^2 | \tilde{q} \rangle|^2$, an η^4 scaling means the amplitude scales as η^2 , i.e., the first-order ($O(\eta)$) amplitude vanishes and the leading contribution is second-order. (In the exact single-channel model with inverse-square perturbation of Sec. VC, the forbidden amplitude vanishes at *all* orders; the residual η^4 weight visible

in Fig. 2 arises from working in the *unperturbed* basis rather than the exact s_η basis.) The deviations from η^4 at larger η are expected from higher-order terms in the unperturbed-basis expansion. This provides independent confirmation of the analytic result (34).

VII. FINITE-TEMPERATURE SUM-RULE ESTIMATE

At finite temperature, multiple radial levels within a channel are thermally populated. The sum-rule centroid (28) assigns each level q a shift $\delta\omega_{\text{cen}}^{(q)}/(2\omega) = \kappa_s/(2Q)$. We stress that Eq. (28) is not the exact spectral line position of the single-channel Hamiltonian $H_{s,\eta}$ (whose spectrum stays at $\pm 2\omega$ exactly, Eq. (25)), but the sum-rule centroid for the channel derived in Sec. VD. A natural thermal average of these per-level values is obtained by weighting each level by its Boltzmann factor $p_q \propto x^q$ and its upward oscillator strength $U_{s,q}$ [15, 16]. (In the retarded susceptibility $\chi''(\omega)$, detailed balance introduces the factor $(p_q - p_{q+1}) = (1-x)p_q$; because all lines sit at the same frequency 2ω , this common factor $(1-x)$ cancels in a normalized centroid.) The resulting thermal centroid within channel s is

$$\frac{\delta\omega_{\text{cen}}^{(s)}(T)}{2\omega} = \frac{\kappa_s}{2} \langle Q^{-1} \rangle_T, \quad (36)$$

where

$$\langle Q^{-1} \rangle_T \equiv \frac{\sum_{q \geq 0} U_{s,q} Q^{-1} x^q}{\sum_{q \geq 0} U_{s,q} x^q}, \quad x \equiv e^{-2\hbar\omega/(k_B T)}. \quad (37)$$

The weight $U_{s,q}$ is the correct choice for a positive-frequency centroid of the positive-frequency spectrum: each physical transition $q \rightarrow q+1$ is counted once, weighted by its upward oscillator strength from the occupied level q . (Using the total unsigned strength $W_{s,q} = U_{s,q} + D_{s,q}$ would double-count: the same transition $q \leftrightarrow q+1$ would appear once through $U_{s,q}$ in level q 's weight and again through $D_{s,q+1} = U_{s,q}$ in level $q+1$'s weight, but assigned different centroid factors Q_q^{-1} and Q_{q+1}^{-1} .)

This is a thermal average *within a single channel*; the factor $x^q = e^{-\beta(E_{s,q} - E_{s,0})}$ is the canonical Boltzmann weight within the radial ladder and does not presume noninteracting single-particle statistics. The connection to the many-body breathing response requires summation over channels weighted by their many-body occupation (see Sec. X).

The denominator sums to a closed rational function:

$$\sum_{q \geq 0} U_{s,q} x^q = \frac{(s+1) + (1-s)x}{(1-x)^3}. \quad (38)$$

The numerator admits a compact representation via the Lerch transcendent $\Phi(x, \nu, a) \equiv \sum_{k \geq 0} x^k / (k+a)^\nu$ [38,

39]:

$$\sum_{q \geq 0} \frac{U_{s,q}}{Q} x^q = \frac{x}{2(1-x)^2} + \frac{s+3}{4(1-x)} - \frac{s^2-1}{8} \Phi(x, 1, \frac{s+1}{2}).$$

The limits of the thermal average are:

$$\langle Q^{-1} \rangle_T \rightarrow \begin{cases} (s+1)^{-1} & T \rightarrow 0, \\ (1-x)/4 \simeq \hbar\omega/(2k_B T) & T \rightarrow \infty. \end{cases}$$

At low temperature, only $q = 0$ is occupied, and $U_{s,0}/(2 \cdot 0 + s + 1) = (s+1)/(s+1) = 1$, giving $\langle Q^{-1} \rangle_T = 1/(s+1)$. At high temperature, the dominant levels have $q \sim k_B T / (2\hbar\omega)$, so $Q^{-1} \sim \hbar\omega / (k_B T)$ and the estimate decays as $1/T$. Physically, heating populates higher radial levels where the centroid contribution is suppressed by the Q^{-1} factor (Fig. 1b).

VIII. ROBUSTNESS UNDER WEAK ANISOTROPY

Real traps are never perfectly isotropic. We now discuss the extent to which the key results survive under weak anisotropy.

Let the squared trap frequencies be $\omega_i^2 = \omega^2(1 + \epsilon_i)$ with $\sum_i \epsilon_i = 0$ and $|\epsilon_i| \ll 1$. The anisotropic perturbation can be written as

$$\delta V = \frac{1}{2} m \omega^2 \epsilon_2 R^2 \hat{Q},$$

where $\epsilon_2 \equiv (\sum_i \epsilon_i^2)^{1/2}$ is the overall anisotropy magnitude and $\hat{Q}(\Omega) \equiv \epsilon_2^{-1} \sum_i \epsilon_i r_i^2 / R^2$ is a traceless angular operator. The key structural point is that δV factors into a radial piece (R^2) times an angular piece (\hat{Q}). Consequently, the radial matrix elements of δV have exactly the same three-term tridiagonal structure as R^2 itself: Within a single channel ($s' = s$), the radial part of δV inherits the tridiagonality of R^2 :

$$\langle s, q' | \delta V | s, q \rangle = \frac{1}{2} m \omega^2 a_{\text{ho}}^2 \epsilon_2 \langle s | \hat{Q} | s \rangle \langle q' | R^2 / a_{\text{ho}}^2 | q \rangle_s,$$

where $\langle q' | R^2 / a_{\text{ho}}^2 | q \rangle_s$ is the fixed- s tridiagonal matrix from Eq. (11). For cross-channel matrix elements ($s' \neq s$), the radial wavefunctions depend on different values of the channel parameter, and the R^2 matrix element $\langle q'(s') | R^2 | q(s) \rangle$ is not in general tridiagonal. We do not evaluate these cross-channel radial overlaps here.

This has two consequences and one important limitation.

First, *within a single channel*, the anisotropy perturbation does not break the radial selection rule $\Delta q = \pm 1$, because the radial part of δV inherits the tridiagonality of R^2 .

Second, the anomaly perturbation *by itself* preserves $\Delta q = \pm 1$ (Eq. (35)), as proved in Sec. VI.

The limitation is that the anisotropy mixes different angular channels through $\langle s' | \hat{Q} | s \rangle \neq 0$ for $s' \neq s$. Once

channels are mixed, the eigenstates are no longer pure $|s, q\rangle$ states, and the notion of “within a single channel” becomes approximate. Our zero-leakage proof relied on the specific matrix elements of \hat{C} *within* a single channel; for the combined anomaly-plus-anisotropy perturbation, the intermediate states in the perturbative sums include other-channel contributions whose contact structure is different. We have not proved that the cancellation persists for the combined perturbation, and at $O(\varepsilon_A \varepsilon_2)$ mixed terms may appear.

For weak anisotropy ($|\varepsilon_2| \ll 1$), the channel mixing is itself a small correction, so the within-channel results are expected to hold approximately. A quantitative analysis of the combined anomaly–anisotropy case is left for future work [10, 16–18, 40].

IX. CALIBRATION AND EXPERIMENTAL CONNECTION

A. Calibration procedure

The exact single-channel result of this paper is Eq. (25): the monopole line remains at 2ω exactly within the single-channel model. The sum-rule estimate (28) is derived by substituting single-channel quantities into the sum-rule bound of Gao and Yu (Sec. V D); the coefficient κ_s defined in (29) involves the contact C_s and its scale derivative, which are not computed from the single-channel model alone.

A practical route is to calibrate κ_s from a low-temperature or $q=0$ measurement of the breathing frequency. For the two-body problem, the identification $C_s = \lambda_s/s$ is exact; for many-body experiments where a single channel dominates, the fitted κ_s absorbs the (unknown) channel-weighting structure, finite-range effects, and other contributions. With κ_s calibrated from a single point, the testable predictions are the *functional form* of the q -dependence ($1/Q$ scaling) and the T -dependence (the shape of the $\langle Q^{-1} \rangle_T$ curve, including the crossover from the low- T plateau to the $1/T$ tail). Agreement or disagreement with these functional forms tests the single-channel sum-rule framework independently of the overall magnitude.

Note that a single measurement at $q=0$ fixes κ_s directly; separating the contact and curvature contributions requires either an independent estimate or a second measurement in a different channel.

B. Worked example ($s = 2$)

For the commonly used $s = 2$ channel at $q=0$ ($Q = 3$), Eq. (28) gives

$$\frac{\delta\omega_{2,0}^{\text{SR}}}{2\omega} = \frac{\kappa_2}{6}.$$

A single reference measurement at $q=0$ therefore fixes $\kappa_2 = 6 [\delta\omega^{\text{SR}}/(2\omega)]_{q=0, s=2}$. The estimate for any q in the same channel is then

$$\frac{\delta\omega_{2,q}^{\text{SR}}}{2\omega} = \frac{\kappa_2}{2Q}, \quad Q = 2q + 3,$$

and the thermal average follows from (36) with no additional free parameters.

Representative 2D ${}^6\text{Li}$ measurements report fractional shifts $|\delta\omega|/(2\omega) \sim 1\%–5\%$ [12–14]. For $s=2$, $q=0$, this corresponds to $|\kappa_2| \approx 0.06–0.30$.

C. Finite range and quasi-2D

Quasi-2D realizations induce an effective range that weakens the anomaly relative to ideal 2D [32, 33]. In the sum-rule centroid for the channel (28), these effects enter through the contact C_s and its scale derivative, which acquire geometry dependence. This is absorbed into a geometry-dependent coefficient, $\kappa_s \rightarrow \kappa_s(r_{\text{eff}}, \ell_z)$, so that

$$\frac{\delta\omega_{s,q}^{\text{SR}}}{2\omega} = \frac{\kappa_s(r_{\text{eff}}, \ell_z)}{2Q}.$$

The Q^{-1} structure is preserved because it originates from the Q -proportional expectation value of R^2 , which is a single-channel kinematic result independent of the interaction details. A calibration at $q=0$ in the same geometry then fixes the remaining q - and T -dependence within that channel [32, 33].

X. DISCUSSION AND OUTLOOK

A. Summary of results

We have shown that the $1/R^2$ perturbation within a single hyperangular channel of a harmonically trapped system is absorbed exactly into a shift of the channel parameter, $s \rightarrow s_\eta$ (Eq. (21)), so the single-channel model remains a harmonic oscillator with a shifted inverse-square term at all orders. A classical identity for products of associated Laguerre polynomials [23, 24] provides closed-form matrix elements. The exact consequences are:

1. *Exact 2ω spacing* (Eq. (25)): radial gaps remain $2\hbar\omega$ exactly, R^2 stays tridiagonal in the exact eigenbasis, and no monopole spectral weight appears at forbidden frequencies at any order in η .
2. *q -independent diagonal matrix element* (Eq. (10)): $\langle \hat{C} \rangle_{s,q} = \lambda_s/s$ for all q , where \hat{C} is the $1/R^2$ -weighted single-channel operator defined in Sec. II.
3. *Independent first-order algebraic proof* (Eqs. (34)–(35)): the first-order cancellation of forbidden spectral weight is proved by an explicit term-by-term

cancellation in which the q - and s -dependence drops out of each pair, confirmed by exact diagonalization (Fig. 2).

Substituting the exact single-channel quantities into the m_1/m_{-1} sum-rule bound of Gao and Yu [19] yields a sum-rule estimate with Q^{-1} scaling (Eq. (28)) and an explicit coefficient (29). Its finite-temperature average (Eq. (36)), using upward oscillator strengths $U_{s,q}$ as the correct positive-frequency weights [15], has a low- T plateau and $1/T$ high- T tail with closed-form expressions involving the Lerch transcendent [38].

The Laguerre identity, the ratio $I_{s-1}/I_s = 1/s$, the exact solvability, and the selection-rule preservation hold for any real $s > 0$ and thus apply formally in three dimensions upon $s \rightarrow \alpha$; the sum-rule-estimate interpretation, however, encounters an additional complication in 3D (see below).

B. Single-channel results and the many-body breathing mode

Several layers of interpretation separate the exact single-channel results proved here from a measured many-body breathing frequency.

First, the exact single-channel statement is Eq. (25): the radial spectrum has exact 2ω spacing at all orders in η , and no forbidden spectral weight appears. This is a rigorous consequence of the inverse-square structure of the model Hamiltonian (20).

Second, many-body sum-rule and hydrodynamic approaches [3, 4, 19] relate the breathing-mode shift to the equation of state and contact derivatives. The single-channel sum-rule estimate (28) is derived by inserting exact single-channel quantities (q -independent contact C_s , Q -proportional $\langle R^2 \rangle$) into the sum-rule bound of Gao and Yu. The Q^{-1} structure follows from these two inputs; the overall coefficient κ_s depends on the contact C_s and its scale derivative, which for $N > 2$ are not computed from the single-channel model alone.

Third, the finite- T average (36) is a thermal average of the derived per-level sum-rule estimates within one channel. The actual many-body finite- T response depends on the full density matrix across all channels and on inter-channel couplings. The single-channel formula captures the qualitative behavior (low- T plateau, $1/T$ high- T tail), but its quantitative comparison with experiment requires the inter-channel summation that we do not perform.

The main open problem is therefore the bridge from exact single-channel matrix elements to the full many-body response. For the two-body problem this bridge is trivial for the exact results (matrix elements, selection rule, exact solvability); the sum-rule centroid can be compared with the exact two-body frequency from Busch's solution [31]. For $N > 2$ the bridge requires knowledge of the many-body channel occupation, which depends on the interaction strength and statistics.

C. Outlook

The most direct tests of the exact results derived here are few-body and state-resolved. In optical microtraps or tweezer platforms, where individual motional levels of two atoms can be prepared and probed [41–43], one may test the closed-form matrix elements, the absence of forbidden monopole transitions (exact at all orders within the single-channel model), and the sum-rule centroid (28) against the exact two-body frequency [31].

For many-body experiments, the sum-rule centroid (28) provides a compact one-parameter scheme once a reference point is supplied. In trap units, the high- T slope of $\delta\omega_{\text{cen}}^{(s)}(T)/(2\omega)$ versus $1/(T/T_{\text{ho}})$ is $\kappa_s/4$, while the low- T plateau tends to $\kappa_s/(2(s+1))$. These functional forms are parameter-free once κ_s is calibrated at $T \approx 0$; their agreement or disagreement with a temperature scan of $\omega_B(T)$ —in the spirit of recent precision studies of 2D collective dynamics [44, 45]—would provide a direct test of the single-channel sum-rule framework. Because exact scale invariance implies vanishing bulk viscosity, any dissipative broadening remains a sensitive symmetry-breaking diagnostic [37, 46].

The Laguerre polynomial identities and the exact solvability extend formally to any real positive parameter, so the integral identities, the exact 2ω radial spacing, and the cancellation mechanism apply formally in three dimensions upon $s \rightarrow \alpha$, where α is the 3D hyperradial parameter [2, 25]: the identity $I_{\alpha-1}/I_\alpha = 1/\alpha$, the off-diagonal matrix element formula (33), the selection-rule preservation (35), and the exact spectrum (23) all hold with s replaced by α . We have verified the selection-rule preservation and the ratio $I_{\alpha-1}/I_\alpha = 1/\alpha$ numerically for non-integer values $\alpha = 0.5, 1.5, 2.5, 3.7$.

What does *not* follow straightforwardly is the physical interpretation in three dimensions. Werner and Castin [26] showed that within an $SO(2,1)$ energy ladder of a trapped 3D gas, the energy derivatives $\partial E/\partial(1/a)$ and $\partial E/\partial r_e$ vary with the ladder index q . This q -dependence of the physical contact correction is incompatible with the q -independent model operator $\langle \hat{C} \rangle_{s,q} = \lambda_s/s$. A genuine three-dimensional breathing-mode application therefore requires a separate derivation that incorporates the q -dependent corrections. At exact 3D unitarity the anomaly piece vanishes ($\varepsilon_A = 0$) [2, 4], and the exact results remain valid and potentially useful as building blocks for a more complete treatment.

In the presence of weak quartic anharmonicity ($V_{\text{ext}} = \frac{1}{2}m\omega^2 r^2 + \kappa r^4$), the anharmonicity breaks the uniform level spacing and can shift the single-channel line independently of the inverse-square perturbation studied here [47]; combining this effect with the anomaly in the many-body sum-rule framework yields a mixed term [4, 16] whose coefficient we have not independently verified within the single-channel model.

-
- [1] L. P. Pitaevskii and A. Rosch, Breathing modes and hidden symmetry of trapped atoms in two dimensions, *Phys. Rev. A* **55**, R853 (1997).
- [2] F. Werner and Y. Castin, Unitary gas in an isotropic harmonic trap: Symmetry properties and applications, *Phys. Rev. A* **74**, 053604 (2006).
- [3] J. Hofmann, Quantum anomaly, universal relations, and breathing mode of a two-dimensional Fermi gas, *Phys. Rev. Lett.* **108**, 185303 (2012).
- [4] E. Taylor and M. Randeria, Apparent low-energy scale invariance in two-dimensional Fermi gases, *Phys. Rev. Lett.* **109**, 135301 (2012).
- [5] Y. Castin, Exact scaling transform for a unitary quantum gas in a time dependent harmonic potential, *C. R. Physique* **5**, 407 (2004).
- [6] Y. Nishida and D. T. Son, Nonrelativistic conformal field theories, *Physical Review D* **76**, 086004 (2007).
- [7] M. Olshanii, H. Perrin, and V. Lorent, Example of a quantum anomaly in the physics of ultracold gases, *Phys. Rev. Lett.* **105**, 095302 (2010).
- [8] E. Taylor and M. Randeria, Erratum: Apparent low-energy scale invariance in two-dimensional Fermi gases, *Phys. Rev. Lett.* **110**, 089904 (2013).
- [9] S. Moroz, Scale-invariant Fermi gas in a time-dependent harmonic potential, *Phys. Rev. A* **86**, 011601 (2012).
- [10] D. S. Lobser, A. E. S. Barentine, E. A. Cornell, and H. J. Lewandowski, Observation of a persistent non-equilibrium state in cold atoms, *Nature physics* **11**, 1009 (2015).
- [11] E. Vogt, M. Feld, B. Fröhlich, D. Pertot, M. Koschorreck, and M. Köhl, Scale invariance and viscosity of a two-dimensional Fermi gas, *Phys. Rev. Lett.* **108**, 070404 (2012).
- [12] M. Holten, L. Bayha, A. C. Klein, P. A. Murthy, P. M. Preiss, and S. Jochim, Anomalous breaking of scale invariance in a two-dimensional Fermi gas, *Phys. Rev. Lett.* **121**, 120401 (2018).
- [13] T. Peppler, P. Dyke, M. Zamorano, I. Herrera, S. Hoinka, and C. J. Vale, Quantum anomaly and 2d–3d crossover in strongly interacting Fermi gases, *Phys. Rev. Lett.* **121**, 120402 (2018).
- [14] P. A. Murthy, N. Defenu, L. Bayha, M. Holten, P. M. Preiss, S. Jochim, and T. Enss, Quantum scale anomaly and spatial coherence in a 2d Fermi superfluid, *Science* **365**, 268 (2019).
- [15] E. Lipparini and S. Stringari, Sum rules and giant resonances in nuclei, *Physics Reports* **175**, 103 (1989).
- [16] S. Stringari, Collective excitations of a trapped bose-condensed gas, *Phys. Rev. Lett.* **77**, 2360 (1996).
- [17] Y. Kagan, E. L. Surkov, and G. V. Shlyapnikov, Evolution of a bose-condensed gas under variations of the confining potential, *Physical Review A* **54**, R1753 (1996).
- [18] Y. Kagan, E. L. Surkov, and G. V. Shlyapnikov, Evolution of a bose gas in anisotropic time-dependent traps, *Physical Review A* **55**, R18 (1997).
- [19] C. Gao and Z. Yu, Breathing mode of two-dimensional atomic Fermi gases in harmonic traps, *Physical Review A* **86**, 043609 (2012).
- [20] B. C. Mulkerin, X.-J. Liu, and H. Hu, Collective modes of a two-dimensional Fermi gas at finite temperature, *Physical Review A* **97**, 053612 (2018).
- [21] U. Toniolo, B. C. Mulkerin, X.-J. Liu, and H. Hu, Breathing-mode frequency of a strongly interacting Fermi gas across the two- to three-dimensional crossover, *Physical Review A* **97**, 063622 (2018).
- [22] V. Bekassy and J. Hofmann, Nonrelativistic conformal invariance in mesoscopic two-dimensional Fermi gases, *Physical Review Letters* **128**, 193401 (2022).
- [23] G. Gasper, Products of terminating ${}_3f_2(1)$ series, *Pacific J. Math.* **56**, 87 (1975).
- [24] H. M. Srivastava, H. A. Mavromatis, and R. S. Allassar, Remarks on some associated Laguerre integral results, *Applied Mathematics Letters* **16**, 1131 (2003).
- [25] Y. Castin, The unitary gas and its symmetry properties, [arXiv:1103.2851](https://arxiv.org/abs/1103.2851) (2011).
- [26] F. Werner and Y. Castin, General relations for quantum gases in two and three dimensions: Two-component fermions, *Phys. Rev. A* **86**, 013626 (2012).
- [27] S. Tan, Energetics of a strongly correlated Fermi gas, *Annals of Physics* **323**, 2952 (2008).
- [28] S. Tan, Large momentum part of a strongly correlated Fermi gas, *Annals of Physics* **323**, 2971 (2008).
- [29] S. Tan, Generalized virial theorem and pressure relation for a strongly correlated Fermi gas, *Annals of Physics* **323**, 2987 (2008).
- [30] E. Braaten and L. Platter, Exact relations for a strongly interacting Fermi gas from the operator product expansion, *Physical Review Letters* **100**, 205301 (2008).
- [31] T. Busch, B.-G. Englert, K. Rzazewski, and M. Wilkens, Two cold atoms in a harmonic trap, *Foundations of Physics* **28**, 549 (1998).
- [32] H. Hu, B. C. Mulkerin, U. Toniolo, L. He, and X.-J. Liu, Reduced quantum anomaly in a quasi-two-dimensional Fermi superfluid: significance of the confinement-induced effective range of interactions, *Physical Review Letters* **122**, 070401 (2019).
- [33] X.-Y. Yin, H. Hu, and X.-J. Liu, Few-body perspective of a quantum anomaly in two-dimensional Fermi gases, *Physical Review Letters* **124**, 013401 (2020).
- [34] G. Szegő, *Orthogonal Polynomials*, 4th ed., American Mathematical Society Colloquium Publications, Vol. 23 (American Mathematical Society, 1975).
- [35] F. Dalfovo, S. Giorgini, L. P. Pitaevskii, and S. Stringari, Theory of Bose-Einstein condensation in trapped gases, *Rev. Mod. Phys.* **71**, 463 (1999).
- [36] S. Chiacchiera, D. Davesne, T. Enss, and M. Urban, Damping of the quadrupole mode in a two-dimensional Fermi gas, *Physical Review A* **88**, 053616 (2013).
- [37] D. T. Son, Vanishing bulk viscosities and conformal invariance of the unitary Fermi gas, *Physical Review Letters* **98**, 020604 (2007).
- [38] L. Lewin, *Polylogarithms and Associated Functions* (North-Holland, 1981).
- [39] A. Erdélyi, W. Magnus, F. Oberhettinger, and F. G. Tricomi, *Higher Transcendental Functions, Vol. I* (McGraw–Hill, 1953).
- [40] D. Guéry-Odelin, F. Zambelli, J. Dalibard, and S. Stringari, Collective oscillations of a classical gas confined in harmonic traps, *Physical Review A* **60**, 4851 (1999).
- [41] F. Serwane, G. Zürn, T. Lompe, T. B. Ottenstein, A. N. Wenz, and S. Jochim, Deterministic preparation of a tun-

- able few-Fermion system, [Science](#) **332**, 336 (2011).
- [42] G. Zürn, F. Serwane, T. Lompe, A. N. Wenz, M. G. Ries, J. E. Bohn, and S. Jochim, Fermionization of two distinguishable Fermions, [Phys. Rev. Lett.](#) **108**, 075303 (2012).
- [43] J. D. Hood, Y. Yu, C. Lin, R. Caldwell, V. Gavryusev, and M. G. Raizen, Multichannel interactions of two atoms in an optical tweezer, [Phys. Rev. Research](#) **2**, 023108 (2020).
- [44] C. He, Z. Ren, B. Song, E. Zhao, J. Lee, Y.-C. Zhang, S. Zhang, and G.-B. Jo, Collective excitations in two-dimensional $su(N)$ Fermi gases with tunable spin, [Physical Review Research](#) **2**, 012028 (2020).
- [45] M. Bohlen, L. Sobirey, N. Luick, H. Biss, T. Enss, T. Lompe, and H. Moritz, Sound propagation and quantum-limited damping in a two-dimensional Fermi gas, [Physical Review Letters](#) **124**, 240403 (2020).
- [46] T. Enss, Bulk viscosity and contact correlations in attractive Fermi gases, [Physical Review Letters](#) **123**, 205301 (2019).
- [47] T. N. de Silva, Breathing mode frequencies of a rotating Fermi gas in the BCS-BEC crossover region, [Physical Review A](#) **78**, 023623 (2008).